A Robust Multi-market Scheduling Strategy for Battery Energy Storage Systems

Sunho Jang
Electrical & Computer Engineering, University of Michigan
Ann Arbor, MI 48105, USA
sunhoj@umich.edu

Siddharth Bhela, Nan Xue
Siemens Technology
Princeton, NJ 08540, USA
{siddharth.bhela,nan.xue}@siemens.com

***Abstract*—In this paper, we propose a novel robust battery energy storage system (BESS) scheduling algorithm that makes offers to multiple ancillary service markets. The proposed algorithm enables BESS to provide frequency regulation and synchronized reserve services while concurrently fulfilling commitments to a long-term capacity market without violating any operational constraints. In particular, the offers to the ancillary service markets scheduled by the proposed algorithm remain valid under any possible frequency regulation signal and synchronized reserve events within the defined uncertainty set. The case study demonstrates that the proposed algorithm is robust to the given uncertainties and outperforms two selected benchmarks.**

***Index Terms*—Battery energy storage system (BESS), robust optimization, ancillary services, long-term capacity market**

I. Introduction

As the penetration of intermittent renewable energy generation continues to surge, the role of battery energy storage systems (BESS) has become important for ensuring grid resiliency. With their rapid ramping capabilities, BESSs can deal with the fluctuations in renewable energy generation by offering various ancillary services, and generate revenues. There is a large body of work on optimal operations of BESSs to maximize revenues through energy arbitrage [1], peak-shaving [2], and frequency regulation [3].

However, scheduling offers to the ancillary services markets is challenging since we cannot precisely predict in advance how much BESS's capacity will be available. This is mainly due to the uncertainty within the net power consumption of a BESS when it is providing an ancillary service, which is governed by some unpredictable signals or events (e.g., frequency regulation signal, synchronized reserve events). This necessitates an algorithm that schedules an appropriate amount of BESS's capacity to each ancillary service market that can be provided as planned for any possible uncertainties.

Several previous studies have proposed robust approaches for BESS energy arbitrage [4] and co-optimization of multiple ancillary service markets [5], [6]. The uncertainty within the frequency regulation signal has been addressed by a scenario-based approach [7] or a chance-constrained approach [8]. Nevertheless, these approaches do not guarantee robustness against the uncertainties within the ancillary services and do not consider the commitment to capacity markets.

In this work, we introduce a novel robust look-ahead BESS scheduling (RLABS) algorithm that is able to derive additional revenue from ancillary service markets while accounting for the long-term BESS commitment to capacity markets. The provided algorithm is robust against uncertainties from the frequency regulation signal and synchronized reserve events so that the BESS can provide the scheduled capacity for any possible uncertainties. In the description of those uncertainties, we utilize the concept of uncertainty budgets to curtail excessive conservatism in the robust algorithm [9].

This paper is organized as follows. Section II introduces RLABS and Section III proposes a tractable reformulation of the original problem. Section IV demonstrates the result of case studies where we compare the proposed algorithm with two benchmarks. Section V provides the conclusion of the paper.

Notation: For sets A and B, $A \times B$ is the cartesian product of them. The notation $(x)^+$ refers to $\max\{x, 0\}$.

II. Problem Formulation

In this section, we introduce RLABS which offers the BESS's capacity to frequency regulation and synchronized reserve markets. We start with models for the BESS, ancillary service markets, and the long-term capacity market which form the constraints and objective function of RLABS. The scheduling is conducted for T discrete time steps with length Δt, indexed by $t \in \mathcal{T} := \{1, \dots, T\}$. Our problem of interest specifically considers a day-ahead hourly scheduling, i.e., $\Delta t = 1$ hour and $T = 24$. All the terms representing powers with subscript t refer to the average power during the time step t.

A. BESS & Microgrid Model

The State of Charge (SoC) of the BESS at time step t is denoted by E_t^{B} and evolves as follows

$$E_{t+1}^{\mathrm{B}} = E_t^{\mathrm{B}} + \eta_c P_t^{\mathrm{C}} - \frac{1}{\eta_d} P_t^{\mathrm{D}} \qquad \forall t \in \mathcal{T}. \tag{1}$$

Here P_t^{C} and P_t^{D} are charging and discharging power at time t, η_c and η_d are charging and discharging efficiencies, respectively. Since it is not possible to charge and discharge simultaneously, the following holds

$$0 \le P_t^{\mathrm{C}} \le \mu_t \overline{P}^{\mathrm{C}} \qquad \forall t \in \mathcal{T} \tag{2}$$

$$0 \le P_t^{\mathrm{D}} \le (1 - \mu_t)\, \overline{P}^{\mathrm{D}} \qquad \forall t \in \mathcal{T}, \tag{3}$$

where $\overline{P}^{\mathrm{C}}$ and $\overline{P}^{\mathrm{D}}$ is the maximum charging and discharging power, respectively, μ_t is 1 if the BESS is charging, and 0 otherwise. The BESS's net power consumption P_t^{N} is defined as

$$P_t^{\mathrm{N}} = P_t^{\mathrm{C}} - P_t^{\mathrm{D}} \qquad \forall t \in \mathcal{T}. \tag{4}$$

The SoC must be kept inside the range $[\underline{E}^{\mathrm{B}}, \overline{E}^{\mathrm{B}}]$:

$$\underline{E}^{\mathrm{B}} \leq E_t^{\mathrm{B}} \leq \overline{E}^{\mathrm{B}} \qquad \forall t \in \mathcal{T} \cup \{T+1\}. \tag{5}$$

In addition, we keep the SoC E_{T+1}^{B} at the end of the horizon to be the same as the initial SoC $E_1^{\mathrm{B}} = E_{\mathrm{i}}$, and hence E_{T+1}^{B} and P_T^{n} satisfy

$$E_1^{\mathrm{B}} = E_{T+1}^{\mathrm{B}} = E_{\mathrm{i}} \tag{6}$$

$$P_T^{\mathrm{N}} = \begin{cases} \eta_d \left(E_{\mathrm{i}} - E_T^{\mathrm{B}}\right) & \text{if } E_T^{\mathrm{B}} \geq E_{\mathrm{i}} \\ \left(E_{\mathrm{i}} - E_T^{\mathrm{B}}\right)/\eta_c & \text{otherwise,} \end{cases} \tag{7}$$

where (7) is the net power consumption at T for E_{T+1}^{B} to be E_{i}. Since P_T^{N} must be between $-\overline{P}^{\mathrm{D}}$ and $\overline{P}^{\mathrm{C}}$, we impose the following constraint on E_T^{B}

$$E_{\mathrm{i}} - \eta_c \overline{P}^{\mathrm{C}} \leq E_T^{\mathrm{B}} \leq E_{\mathrm{i}} + \frac{1}{\eta_d} \overline{P}^{\mathrm{D}}. \tag{8}$$

Assuming the BESS is installed in a microgrid with a solar PV array, we denote by P_t^{G} the power imported from the grid

$$P_t^{\mathrm{G}} = P_t^{\mathrm{N}} + P_t^{\mathrm{PV}} - P_t^{\mathrm{UC}} \qquad \forall t \in \mathcal{T}, \tag{9}$$

where P_t^{PV} and P_t^{UC} are the forecasted PV generation power and load from the microgrid, respectively. The actual values of P_t^{PV} and P_t^{UC} cannot be known in advance and hence they are uncertainties in the look-ahead planning phase. To mitigate the conservatism of RLABS, we employ the concept of uncertainty budget [9] to define the uncertainty sets for them, effectively narrowing them while including all plausible uncertainties:

$$\mathcal{W}^{\mathrm{PV}} = \left\{ \boldsymbol{P}^{\mathrm{PV}} \;\middle|\; P_t^{\mathrm{PV}} \in \left[\underline{P}_t^{\mathrm{PV}}, \overline{P}_t^{\mathrm{PV}}\right], \right. \left. \underline{\Gamma}_t^{\mathrm{PV}} \leq \sum_{k=1}^{t} P_k^{\mathrm{PV}} \leq \overline{\Gamma}_t^{\mathrm{PV}} \;\; \forall t \in \mathcal{T} \right\} \tag{10}$$

$$\mathcal{W}^{\mathrm{UC}} = \left\{ \boldsymbol{P}^{\mathrm{UC}} \;\middle|\; P_t^{\mathrm{UC}} \in \left[\underline{P}_t^{\mathrm{UC}}, \overline{P}_t^{\mathrm{UC}}\right], \right. \left. \underline{\Gamma}_t^{\mathrm{UC}} \leq \sum_{k=1}^{t} P_k^{\mathrm{UC}} \leq \overline{\Gamma}_t^{\mathrm{UC}} \;\; \forall t \in \mathcal{T} \right\}, \tag{11}$$

where the parameters $\underline{P}_t^{\bullet}$, $\overline{P}_t^{\bullet}$ are the bounds, and $\underline{\Gamma}_t^{\bullet}$, $\overline{\Gamma}_t^{\bullet}$ are the uncertainty budgets for each uncertainty. The bounds on P_t^{PV} and P_t^{UC} are assumed to be forecasted. Uncertainty budgets of those sets can be chosen by investigating the range of cumulative sums of the historical data.

B. Ancillary Service & Long-term Capacity Markets

We consider a scenario in which the BESS is committed to a long-term capacity market. This requires that when the Independent System Operator (ISO) calls upon the BESS for a certain time period (typically during peak demand periods), it must be fully charged to $\overline{E}^{\mathrm{B}}$ and ready to discharge its stored energy to the grid at its maximum discharging power $\overline{P}^{\mathrm{D}}$. To prevent the BESS from being on standby all the time, we assume that the BESS's owner uses a service from a third-party company that provides an accurate time window during which the BESS will be called upon. This approach frees up the BESS owner to make additional revenue from offers to ancillary service markets during times when a call from the ISO is not anticipated. In this work, we consider two ancillary service markets: frequency regulation and synchronized reserve markets.

Suppose that the BESS is expected to be called upon at the time step $t_{\mathrm{F}} \in \mathcal{T}$ and discharge at its maximum power $\overline{P}^{\mathrm{D}}$ during the set of time steps $\mathcal{T}_{\mathrm{F}} \subseteq \mathcal{T}$. Since the demand during the last hour of the day (from 11 p.m. to 12 a.m.) is typically not at its peak for the day-ahead planning, we assume that $\mathcal{T}_{\mathrm{F}}$ does not include the final time step T of the planning horizon. Then, the following must hold:

$$E_{t_{\mathrm{F}}}^{\mathrm{B}} = \overline{E}^{\mathrm{B}} \tag{12}$$

$$P_t^{\mathrm{N}} = -\overline{P}^{\mathrm{D}} \qquad \forall t \in \mathcal{T}_{\mathrm{F}}. \tag{13}$$

For the BESS to be fully charged at t_{F}, the net power consumption at $t_{\mathrm{F}} - 1$ must be

$$P_{t_{\mathrm{F}}-1}^{\mathrm{N}} = \left(\overline{E}^{\mathrm{B}} - E_{t_{\mathrm{F}}-1}\right)/\eta_c. \tag{14}$$

Since $P_{t_{\mathrm{F}}-1}^{\mathrm{N}}$ cannnot be larger than $\overline{P}^{\mathrm{C}}$, we must impose the following constraint on the SoC at $t_{\mathrm{F}} - 1$

$$E_{t_{\mathrm{F}}-1}^{\mathrm{B}} \geq \overline{E}^{\mathrm{B}} - \eta_c \overline{P}^{\mathrm{C}}. \tag{15}$$

Note that the BESS's net power consumption must be manually controlled during the time steps in $\mathcal{T}_{\mathrm{F}}^{+} := \mathcal{T}_{\mathrm{F}} \cup \{t_{\mathrm{F}} - 1, T\}$ as described in (7), (13), and (14). Thus, we make an offer to one of the frequency regulation and synchronized reserve markets only for the time steps in $\mathcal{T}_{\mathrm{S}} := \mathcal{T} \setminus \mathcal{T}_{\mathrm{F}}^{+}$.

While the BESS is providing frequency regulation service, its net power consumption must follow the frequency regulation signal from the ISO. To capture the feature of the regulation signal that is issued in a shorter period (e.g., 2 seconds in PJM) than Δt, we define sub-intervals that break each time step t into D pieces with length $\Delta d := \Delta t / D$, indexed by d. We denote the frequency regulation signal at each sub-interval by $s_{t,d} \in [-1, 1]$. We denote by $s_t := \sum_{d=1}^{D} s_{t,d}/D$ the average of the frequency regulation signal during the time step t, and let $\boldsymbol{s} := \{s_1, \ldots, s_T\}$. Then, the average net power consumption of the BESS at each time step is as follows:

$$P_t^{\mathrm{N}} = P_t^{\mathrm{B}} - s_t P_t^{\mathrm{FR}} \tag{16}$$

where P_t^{B} is the set-point power, which is equal to the BESS's net power consumption when the regulation signal is 0, and

P_t^{FR} is the offered regulation capability. The actual real-time BESS's net power consumption at each sub-interval varies by $s_{t,d}$, and will be presented in Section III.

For the synchronized reserve market, we denote by $r_{t,d} \in [0,1]$ the fraction of reserve actually called upon by the ISO, which is referred to as *utilization rate*, and also $r_t := \sum_{d=1}^{D} r_{t,d}/D$ and $\boldsymbol{r} := \{r_1, \dots, r_T\}$. The BESS's average net power consumption while providing synchronized reserve is

$$P_t^{\mathrm{N}} = P_t^{\mathrm{B}} - r_t P_t^{\mathrm{SR}} \tag{17}$$

where P_t^{SR} is the offered reserve capacity. Here, P_t^{B} is equal to the BESS's net power consumption when there is no synchronized reserve event.

Due to the operational limit, the frequency regulation capability P_t^{FR} and the reserve capacity P_t^{SR} cannot be larger than $\overline{P}^{\mathrm{C}} + \overline{P}^{\mathrm{D}}$. Also, the BESS makes an offer to only one of the frequency regulation and synchronized reserve markets. Thus, we impose the following constraints:

$$0 \leq P_t^{\mathrm{FR}} \leq \alpha_t \left(\overline{P}^{\mathrm{C}} + \overline{P}^{\mathrm{D}}\right) \qquad \forall t \in \mathcal{T}_{\mathrm{S}} \tag{18}$$

$$0 \leq P_t^{\mathrm{SR}} \leq \beta_t \left(\overline{P}^{\mathrm{C}} + \overline{P}^{\mathrm{D}}\right) \qquad \forall t \in \mathcal{T}_{\mathrm{S}} \tag{19}$$

$$0 \leq \alpha_t + \beta_t \leq 1 \qquad \forall t \in \mathcal{T}_{\mathrm{S}} \tag{20}$$

where α_t and β_t are binary variables indicating offers to the frequency regulation and synchronized reserve markets, respectively. Since either P_t^{FR} or P_t^{SR} must be zero, we can integrate (16) and (17) into

$$P_t^{\mathrm{N}} = P_t^{\mathrm{B}} - s_t P_t^{\mathrm{FR}} - r_t P_t^{\mathrm{SR}} \quad \forall t \in \mathcal{T}_{\mathrm{S}}. \tag{21}$$

The maximum charging and discharging power at each sub-interval during the ancillary services (i.e., when $s_{t,d} = 1$ or -1, and $r_{t,d} = 0$ or 1) must be between $\overline{P}^{\mathrm{C}}$ and $\overline{P}^{\mathrm{D}}$:

$$P_t^{\mathrm{B}} + P_t^{\mathrm{FR}} \leq \overline{P}^{\mathrm{C}} \qquad \forall t \in \mathcal{T}_{\mathrm{S}} \tag{22}$$

$$-P_t^{\mathrm{B}} + P_t^{\mathrm{FR}} + P_t^{\mathrm{SR}} \leq \overline{P}^{\mathrm{D}} \qquad \forall t \in \mathcal{T}_{\mathrm{S}}. \tag{23}$$

The frequency regulation signal and utilization rate cannot be known in the look-ahead scheduling phase and hence $\boldsymbol{s}$ and $\boldsymbol{r}$ are uncertain. We employ the concept of uncertainty budget [9] to define uncertainty sets for $\boldsymbol{s}$ and $\boldsymbol{r}$ as well:

$$\mathcal{W}^{\bullet} = \left\{ \bullet \;\middle|\; \bullet_t \in [\underline{\bullet}, \overline{\bullet}], \; \underline{\Gamma}_t^{\bullet} \leq \sum_{k=1}^{t} \bullet_k \leq \overline{\Gamma}_t^{\bullet} \quad \forall t \in \mathcal{T} \right\} \tag{24}$$

where $\bullet \in \{\boldsymbol{s}, \boldsymbol{r}\}$, and $\underline{\bullet}$, $\overline{\bullet}$ are the bounds on the uncertainties at each time step, and $\underline{\Gamma}_t^{\bullet}$, $\overline{\Gamma}_t^{\bullet}$ are the uncertainty budgets. We can obtain these bounds and uncertainty budgets for each uncertainty from historical data. We gather all the uncertainties $\boldsymbol{w} := (\boldsymbol{s}^\top, \boldsymbol{r}^\top, \boldsymbol{P}^{\mathrm{PV}\top}, \boldsymbol{P}^{\mathrm{UC}\top})^\top$ and define uncertainty set $\mathcal{W} := \mathcal{W}^{\mathrm{s}} \times \mathcal{W}^{\mathrm{r}} \times \mathcal{W}^{\mathrm{PV}} \times \mathcal{W}^{\mathrm{UC}}$.

C. Cost

The cost function of RLABS includes four components: energy charge, peak demand charge, ancillary service revenues, and BESS degradation cost. The energy charge is paid to the utility given by

$$J^{\mathrm{E}} = \pi^{\mathrm{E}} \sum_{t=1}^{T} P_t^{\mathrm{G}} \cdot \Delta t, \tag{25}$$

where π^{E} is the fixed-rate cost for unit energy contracted with the utility.

We also consider the peak demand charge that is proportional to the maximum imported power P_t^{G} during the prediction horizon:

$$J^{\mathrm{DC}} = \pi^{\mathrm{DC}} \max_{t \in \mathcal{T}} P_t^{\mathrm{G}}. \tag{26}$$

Note that the prediction horizon for RLABS is usually shorter than the actual billing period (practically a month), and the precise cost might not be precisely included in the cost function. However, by incorporating the peak demand charge J^{DC} with a suitably estimated unit cost π^{DC} from multiple simulations, we can effectively reduce the total cost for the actual billing cycle.

The revenue from each ancillary service market is proportional to P_t^{FR} and P_t^{SR}:

$$J^{\mathrm{AC}} = \sum_{t=1}^{T} \pi_t^{\mathrm{FR}} P_t^{\mathrm{FR}} + \pi_t^{\mathrm{SR}} P_t^{\mathrm{SR}}, \tag{27}$$

where π_t^{FR} and π_t^{SR} are the forecasted day-ahead unit power price for the frequency regulation market and the synchronized reserve market, respectively.

Lastly, we include a BESS degradation cost leveraged in many previous works, e.g., [7], where the cost is proportional to the absolute value of the net power consumption P_t^{N}:

$$J^{\mathrm{BD}} = \pi^{\mathrm{BD}} \sum_{t=1}^{T} \left| P_t^{\mathrm{N}} \right|. \tag{28}$$

Here, π^{BD} is the unit battery degradation cost. Then, the total cost J^{T} is

$$J^{\mathrm{T}} = J^{\mathrm{E}} + J^{\mathrm{DC}} - J^{\mathrm{AC}} + J^{\mathrm{BD}}. \tag{29}$$

D. Robust Look-ahead scheduling optimization

The cost function of a robust optimization is usually the maximum of the objective function with respect to the uncertainties. However, we found that it is non-trivial to get a tractable closed-form expression of $\max_{\boldsymbol{w} \in \mathcal{W}} J^{\mathrm{T}}$. Instead, RLABS leverages the nominal cost $\tilde{J}^{\mathrm{T}}$ that is obtained under the assumption that the uncertainties s_t and r_t are equal to their nominal values $\tilde{s}$ and $\tilde{r}$, respectively; we determine the nominal values as the average value of each frequency regulation signal and utilization rate from the historical data. The average of the uncertainties during the horizon $\mathcal{T}$ is usually close to their nominal values, and hence $\tilde{J}^{\mathrm{T}}$ can reasonably approximate the actual cost J^{T}.

Suppose that $\tilde{E}_t$, $\tilde{P}_t^{\mathrm{G}}$, $\tilde{P}_t^{\mathrm{N}}$, $\tilde{P}_t^{\mathrm{C}}$, $\tilde{P}_t^{\mathrm{D}}$, $\tilde{\mu}_t$ are the nominal values of their corresponding variables under the nominal frequency regulation signal $\tilde{\boldsymbol{s}} := (\tilde{s}, \dots, \tilde{s})$ and utilization rate $\tilde{\boldsymbol{r}} := (\tilde{r}, \dots, \tilde{r})$, which are obtained by incorporating the following constraints:

$$\begin{aligned} &(1)-(14) \text{ with } E_t^{\mathrm{B}}, P_t^{\mathrm{G}}, P_t^{\mathrm{N}}, P_t^{\mathrm{C}}, P_t^{\mathrm{D}}, \mu_t, s_t, r_t \\ &\quad \text{alternated to } \tilde{E}_t^{\mathrm{B}}, \tilde{P}_t^{\mathrm{G}}, \tilde{P}_t^{\mathrm{N}}, \tilde{P}_t^{\mathrm{C}}, \tilde{P}_t^{\mathrm{D}}, \tilde{\mu}_t, \tilde{s}, \tilde{r} \end{aligned} \tag{30}$$

The nominal value of each cost component $\tilde{J}^{\mathrm{E}}$, $\tilde{J}^{\mathrm{DC}}$, $\tilde{J}^{\mathrm{BD}}$, and the total cost $\tilde{J}^{\mathrm{T}}$ are also obtained by imposing

$$\begin{aligned} &(25)-(29) \text{ with } J^{\mathrm{E}}, J^{\mathrm{DC}}, J^{\mathrm{BD}}, J^{\mathrm{T}}, P_t^{\mathrm{G}}, P_t^{\mathrm{N}} \\ &\quad \text{alternated to } \tilde{J}^{\mathrm{E}}, \tilde{J}^{\mathrm{DC}}, \tilde{J}^{\mathrm{BD}}, \tilde{J}^{\mathrm{T}}, \tilde{P}_t^{\mathrm{G}}, \tilde{P}_t^{\mathrm{N}} \end{aligned} \tag{31}$$

Then, RLABS is formulated as follows

$$\begin{aligned} \min_{P_t^{\mathrm{B}}, P_t^{\mathrm{FR}}, P_t^{\mathrm{SR}}, \alpha_t, \beta_t} \quad & \max_{\boldsymbol{P}^{\mathrm{PV}} \in \mathcal{W}^{\mathrm{PV}}, \boldsymbol{P}^{\mathrm{UC}} \in \mathcal{W}^{\mathrm{UC}}} \tilde{J}^{\mathrm{T}} \\ \text{s.t. } & (1)-(23), (30)-(31) \qquad \forall \boldsymbol{w} \in \mathcal{W} \\ & (12)-(15) \qquad \forall \boldsymbol{w} \in \mathcal{W} \quad \text{if } \mathcal{T}_{\mathrm{F}} \neq \phi \end{aligned} \tag{32}$$

Note that all the other variables not listed as the decision variables are dependent variables. The constraints (12) - (15) are imposed only when the full capacity call from the ISO is expected, i.e., $\mathcal{T}_{\mathrm{F}} \neq \phi$. Since the BESS's net power consumption P_t^{N} is uncertain for $t \in \mathcal{T}_{\mathrm{S}}$ as is described in (21) due to uncertain s_t and r_t, the SoC E_t^{B} depends on the uncertainty $\boldsymbol{w}$ except for $t = t_{\mathrm{F}}$ and $T+1$. Hence, RLABS finds the decision variables that satisfy the inequalities on E_t^{B} (5), (8) and (15) for all $\boldsymbol{w} \in \mathcal{W}$. However, the number of possible uncertainties is infinite so we need to reformulate the original RLABS into a problem with a finite number of constraints.

III. Reformulation of RLABS

In this section, we propose a reformulation of the original RLABS (32). We first derive a sufficient condition for (5),(8), and (15) to hold for all uncertainties $\boldsymbol{w} \in \mathcal{W}$ by leveraging bounds on E_t^{B} and Lagrange dual functions. Subsequently, we construct a reformulation by incorporating sufficient conditions as constraints.

We first derive bounds on E_t^{B} as demonstrated in the following proposition.

Proposition 1. *Suppose that P_t^{U} is an auxiliary variable such that*

$$P_t^{\mathrm{U}} \geq \left(-P_t^{\mathrm{B}} + \overline{s} P_t^{\mathrm{FR}} + \overline{r} P_t^{\mathrm{SR}}\right)^+ \qquad \forall t \in \mathcal{T}, \tag{33}$$

E_t^{l} and E_t^{u} are as follows:

$$E_{t+1}^{\mathrm{l}} = E_1^{\mathrm{B}} + \sum_{k=1}^{t} \eta_c P_k^{\mathrm{N}} - \left(\frac{1}{\eta_d} - \eta_c\right) P_k^{\mathrm{U}} \quad \forall t \in \mathcal{T} \tag{34}$$

$$E_{t+1}^{\mathrm{u}} = E_1^{\mathrm{B}} + \sum_{k=1}^{t} \eta P_k^{\mathrm{N}} \quad \forall t \in \mathcal{T} \tag{35}$$

where η is a constant in range $[\eta_c, 1/\eta_d]$. Then, E_t^B is in the range $[E_t^{\mathrm{l}}, E_t^{\mathrm{u}}]$ for all $t \in \mathcal{T} \cup \{t+1\}$.

Proof. The inequality $E_t^{\mathrm{B}} \leq E_t^{\mathrm{u}}$ has already been proved in [10]. Hence, we show only the lower bound condition $E_t^{\mathrm{l}} \leq E_t^{\mathrm{B}}$.

First, P_t^{U} is larger than P_t^{D} for any $t \in \mathcal{T}$ by its definition. Now, we show $E_t^{\mathrm{l}} \leq E_t^{\mathrm{B}}$ by mathematical induction for any $t \leq T$. We first get $E_1^{\mathrm{l}} \leq E_1^{\mathrm{B}}$ from (34) so the statement holds for $t = 1$. Now suppose that $E_t^{\mathrm{l}} \leq E_t^{\mathrm{B}}$ holds. Then, we obtain the following for any $t \leq T$:

$$\begin{aligned} E_{t+1}^{\mathrm{B}} &= E_1^{\mathrm{B}} + \sum_{k=1}^{t-1} \eta_c P_k^{\mathrm{C}} - \frac{1}{\eta_d} P_k^{\mathrm{D}} \\ &= E_1^{\mathrm{B}} + \sum_{k=1}^{t-1} \eta_c \left(P_k^{\mathrm{C}} - P_k^{\mathrm{D}}\right) - \left(\frac{1}{\eta_d} - \eta_c\right) P_k^{\mathrm{D}} \\ &\geq E_1^{\mathrm{l}} + \sum_{k=1}^{t-1} \eta_c P_k^{\mathrm{N}} - \left(\frac{1}{\eta_d} - \eta_c\right) P_k^{\mathrm{U}} = E_{t+1}^{\mathrm{l}}. \end{aligned} \tag{36}$$

By the principle of mathematical induction, $E_t^{\mathrm{l}} \leq E_t^{\mathrm{B}}$ holds for all $t \leq T+1$.

Thus, the statement of the proposition holds. □

According to Proposition 1, inequalities (5), (8) and (15) hold for all $\boldsymbol{w} \in \mathcal{W}$ if the following conditions hold:

$$\min_{\boldsymbol{w} \in \mathcal{W}} E_t^{\mathrm{l}} \geq \underline{E}^{\mathrm{B}}, \ \max_{\boldsymbol{w} \in \mathcal{W}} E_t^{\mathrm{u}} \leq \overline{E}^{\mathrm{B}} \qquad \forall t \in \mathcal{T} \setminus \{t_{\mathrm{F}}\} \tag{37}$$

$$\min_{\boldsymbol{w} \in \mathcal{W}} E_T^{\mathrm{l}} \geq E_{\mathrm{i}} - \eta_c \overline{P}^{\mathrm{C}}, \ \max_{\boldsymbol{w} \in \mathcal{W}} E_T^{\mathrm{u}} \leq E_{\mathrm{i}} + \frac{\overline{P}^{\mathrm{D}}}{\eta_d} \tag{38}$$

$$\min_{\boldsymbol{w} \in \mathcal{W}} E_{t_{\mathrm{F}}-1}^{\mathrm{l}} \geq \overline{E}^{\mathrm{B}} - \eta_c \overline{P}^{\mathrm{C}}. \tag{39}$$

We again derive a sufficient condition of (37), (38) and (39). Let $g_t^{\mathrm{l}}(\boldsymbol{\lambda}_t^{\mathrm{l}})$ and $g_t^{\mathrm{u}}(\boldsymbol{\lambda}_t^{\mathrm{u}})$ be the Lagrange dual functions of $\min_{\boldsymbol{w} \in \mathcal{W}} E_t^{\mathrm{l}}$ and $\max_{\boldsymbol{w} \in \mathcal{W}} E_t^{\mathrm{u}}$, where $\boldsymbol{\lambda}_t^{\mathrm{l}}$ and $\boldsymbol{\lambda}_t^{\mathrm{u}}$ are the vectors composed of the Lagrange multipliers, respectively. These functions are linear functions of the Lagrange multipliers.

By the property of Lagrange dual functions, we get

$$g_t^{\mathrm{l}}\left(\boldsymbol{\lambda}_t^{\mathrm{l}}\right) \leq \min_{\boldsymbol{w} \in \mathcal{W}} E_t^{\mathrm{l}}, \ g_t^{\mathrm{u}}\left(\boldsymbol{\lambda}_t^{\mathrm{u}}\right) \geq \max_{\boldsymbol{w} \in \mathcal{W}} E_t^{\mathrm{u}} \quad \forall \boldsymbol{\lambda}_t^{\mathrm{l}}, \boldsymbol{\lambda}_t^{\mathrm{u}} \geq 0.$$

Thus, the following is a sufficient condition for (37), (38), and (39):

$$\boldsymbol{\lambda}_t^l \geq 0, \quad \boldsymbol{\lambda}_t^u \geq 0, \qquad \forall t \in \mathcal{T} \setminus \{t_{\mathrm{F}}\} \tag{40}$$

$$g_t^{\mathrm{l}}\left(\boldsymbol{\lambda}_t^{\mathrm{l}}\right) \geq \underline{E}^{\mathrm{B}}, \quad g_t^{\mathrm{u}}\left(\boldsymbol{\lambda}_t^{\mathrm{u}}\right) \leq \overline{E}^{\mathrm{B}} \qquad \forall t \in \mathcal{T} \setminus \{t_{\mathrm{F}}\} \tag{41}$$

$$g_T^{\mathrm{l}}\left(\boldsymbol{\lambda}_T^{\mathrm{l}}\right) \geq E_{\mathrm{i}} - \eta_c \overline{P}^{\mathrm{C}}, g_T^{\mathrm{u}}\left(\boldsymbol{\lambda}_T^{\mathrm{u}}\right) \leq E_{\mathrm{i}} + \frac{\overline{P}^{\mathrm{D}}}{\eta_d} \tag{42}$$

$$g_{t_{\mathrm{F}}-1}^{\mathrm{l}}\left(\boldsymbol{\lambda}_{t_{\mathrm{F}}-1}^{\mathrm{l}}\right) \geq \overline{E}^{\mathrm{B}} - \eta_c \overline{P}^{\mathrm{C}}. \tag{43}$$

The inequalities (40)-(42) can be incorporated as linear constraints into an optimization problem.

Now, we reformulate the cost function of the original RLABS (32). Note that $\tilde{P}_t^{\mathrm{G}}$ depends on P_t^{UC} and P_t^{PV}, and hence the approximated energy charge $\tilde{J}^{\mathrm{E}}$ and demand charge $\tilde{J}^{\mathrm{DC}}$ depend on $\boldsymbol{P}^{\mathrm{PV}}$ and $\boldsymbol{P}^{\mathrm{UC}}$. It is obvious that $\tilde{J}^{\mathrm{E}}$ and $\tilde{J}^{\mathrm{DC}}$ are at their maximum with minimum PV generation and maximum load. Thus, the maximum of the sum of $\tilde{J}^{\mathrm{E}}$ and

$\tilde{J}^{\mathrm{DC}}$ is given

$$
\begin{aligned}
\tilde{J}^{\max} &= \max_{\boldsymbol{P}^{\mathrm{PV}} \in \mathcal{W}^{\mathrm{PV}}, \boldsymbol{P}^{\mathrm{UC}} \in \mathcal{W}^{\mathrm{UC}}} \pi^{\mathrm{E}} \sum_{t=1}^{T} \tilde{P}_t^{\mathrm{G}} \cdot \Delta t + \pi^{\mathrm{DC}} \max_{t \in \mathcal{T}} \tilde{P}_t^{\mathrm{G}} \\
&= \pi^{\mathrm{E}} \left(\sum_{t=1}^{T} \tilde{P}_t^{\mathrm{N}} + \overline{\Gamma}_T^{\mathrm{UC}} - \underline{\Gamma}_T^{\mathrm{PV}} \right) \Delta t \\
&\quad + \pi^{\mathrm{DC}} \max_{t \in \mathcal{T}} \left(\tilde{P}_t^{\mathrm{N}} + \overline{P}_t^{\mathrm{UC}} - \underline{P}_t^{\mathrm{PV}} \right).
\end{aligned}
\tag{44}
$$

Thus, the approximated total cost $\tilde{J}^{\mathrm{Tmax}}$ is defined as follows

$$
\tilde{J}^{\mathrm{Tmax}} = \tilde{J}^{\max} - J^{\mathrm{AC}} + \tilde{J}^{\mathrm{BD}}. \tag{45}
$$

Combining the results above, we reformulate the robust look-ahead algorithm as follows

$$
\begin{aligned}
&\min_{P_t^{\mathrm{B}}, P_t^{\mathrm{FR}}, P_t^{\mathrm{SR}} \alpha_t, \beta_t, \boldsymbol{\lambda}_t^{\mathrm{l}}, \boldsymbol{\lambda}_t^{\mathrm{u}}} \tilde{J}^{\mathrm{Tmax}} \\
&\text{s.t. } (18)-(23), (30)-(31), (33)-(35), (40)-(42) \\
&\qquad (43) \qquad\qquad \text{if } \mathcal{T}_{\mathrm{F}} \neq \phi.
\end{aligned}
\tag{46}
$$

Since we incorporate sufficient conditions for the robust version of (5), (8), and (15), an optimal solution for (46) is feasible for the original problem (32) as the subsequent Theorem states.

Theorem 1. *An optimal solution* $\boldsymbol{x}^* = \{P_t^{B*}, P_t^{FR*}, P_t^{SR*}, \alpha_t^*, \beta_t^*\}_{t \in \mathcal{T}_S}$ *obtained from* (46) *is feasible for the original problem* (32).

Proof. It is sufficient to show that (5), (8), and (15) hold for all $\boldsymbol{w}$ in $\mathcal{W}$ under the obtained optimal solution $\boldsymbol{x}^*$. The optimal Lagrange multipliers $\boldsymbol{\lambda}_t^{\mathrm{l}*}$ and $\boldsymbol{\lambda}_t^{\mathrm{u}*}$ from (46) satisfy $\boldsymbol{\lambda}_t^{\mathrm{l}*} \geq 0$, and $\boldsymbol{\lambda}_t^{\mathrm{u}*} \geq 0$ for all $t \in \mathcal{T} \setminus \{t_{\mathrm{F}}\}$ by (40). Suppose that $E_t^{\mathrm{B}*}$ is the BESS's SoC obtained under the optimal decision variables $\boldsymbol{x}^*$. From (41), we get

$$
\begin{aligned}
\min_{\boldsymbol{w} \in \mathcal{W}} E_t^{\mathrm{B}*} &\geq g_t^{\mathrm{l}} \left(\boldsymbol{\lambda}_t^{\mathrm{l}*} \right) \geq \underline{E}^{\mathrm{B}} \\
\max_{\boldsymbol{w} \in \mathcal{W}} E_t^{\mathrm{B}*} &\leq g_t^{\mathrm{u}} \left(\boldsymbol{\lambda}_t^{\mathrm{u}*} \right) \leq \overline{E}^{\mathrm{B}}
\end{aligned}
$$

Thus, (5) holds for all $\boldsymbol{w} \in \mathcal{W}$.

Similarly, we can show that (8) and (15) hold for all $\boldsymbol{w} \in \mathcal{W}$ by the constraints (42) and (43). Thus, the statement of the theorem holds. □

Leveraging the linearization technique introduced in [11] for the term $|\tilde{P}_t^{\mathrm{N}}|$ in $\tilde{J}^{\mathrm{BD}}$ and an auxiliary variable for the max term in $\tilde{J}^{\max}$, (46) can be easily reformulated into a Mixed-Integer Linear Programming (MILP) problem.

After the scheduling is done, the battery's power at each sub-interval $P_{t,d}^{\mathrm{N}}$ is determined from (7), (13),(14), and (21):

$$
P_{t,d}^{\mathrm{N}} = \begin{cases}
P_t^{\mathrm{B}*} - s_{t,d} P_t^{\mathrm{FR}*} - r_{t,d} P_t^{\mathrm{SR}*} & \text{if } t \in \mathcal{T}_{\mathrm{S}} \\
\left(\overline{E}^{\mathrm{B}} - E_{t_{\mathrm{F}}-1} \right) / \eta_c & \text{if } t = t_{\mathrm{F}} - 1 \\
-\overline{P}^{\mathrm{D}} & \text{if } t \in \mathcal{T}_{\mathrm{F}}. \\
\eta_d \left(E_T^{\mathrm{B}} - E_{\mathrm{init}} \right) & \text{if } t = T \text{ and } E_T^{\mathrm{B}} \geq E_{\mathrm{i}} \\
\left(E_T^{\mathrm{B}} - E_{\mathrm{i}} \right) / \eta_c & \text{if } t = T \text{ and } E_T^{\mathrm{B}} < E_{\mathrm{i}}
\end{cases}
$$

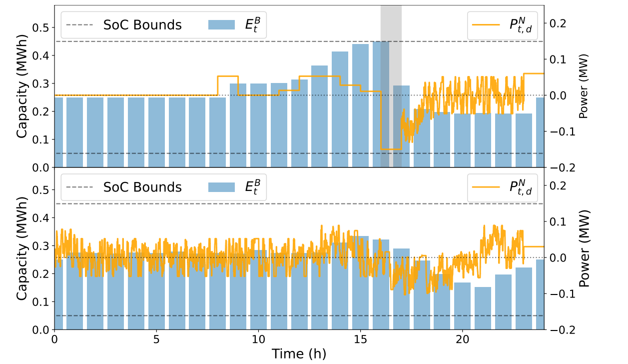

Fig. 1: BESS's SoC E_t^{B} (blue bars) and net power consumption $P_{t,d}^{\mathrm{N}}$ (orange lines) on the 4th day (top) and 7th day (bottom) of the month under RLABS. The grey block indicates the time ($\mathcal{T}_{\mathrm{F}}$) when the BESS's full capacity is called upon.

IV. Experiments

In this section, we compare RLABS with two benchmarks. We run each algorithm for 29 days within a month and compare the total monthly energy charge.

The parameters leveraged for the experiments are written in the footnote[1]. The bounds and nominal values of the frequency regulation signal and the utilization rate are obtained from PJM's regulation data in 2020 [12]. The uncertainty budgets $\underline{\Gamma}_t^{\mathrm{s}}$ and $\overline{\Gamma}_t^{\mathrm{s}}$ are determined as the minimum and maximum cumulative sum from the same data. We leverage solar radiation data from SoDa [13] to generate predicted solar power generation bounds $\underline{P}_t^{\mathrm{PV}}, \overline{P}_t^{\mathrm{PV}}$. The microgrid's load bounds $\underline{P}_t^{\mathrm{UC}}, \overline{P}_t^{\mathrm{UC}}$ are obtained by scaling hourly load data from PJM [14]. Then, we sample P_t^{PV} and P_t^{UC} from uniform distributions over ranges $[\underline{P}_t^{\mathrm{PV}}, \overline{P}_t^{\mathrm{PV}}]$ and $[\underline{P}_t^{\mathrm{UC}}, \overline{P}_t^{\mathrm{UC}}]$, respectively. The uncertainty budgets $\underline{\Gamma}_t^{\mathrm{PV}}$,$\overline{\Gamma}_t^{\mathrm{PV}}$, $\underline{\Gamma}_t^{\mathrm{UC}}$,$\overline{\Gamma}_t^{\mathrm{UC}}$ are chosen as appropriate values. For the forecasted prices of the ancillary service markets π_t^{FR} and π_t^{SR}, we use the prices of PJM's frequency regulation market from June 18th 2023 to July 16th 2023. We assume that the BESS is called upon for its commitment to the long-term capacity market from 4pm-5pm on the 4th day and 7pm-8pm on the 21st day.

Benchmark 1 is a rule-based BESS controller that fully discharges the BESS during $\mathcal{T}_{\mathrm{F}}$ if there is an anticipated call from the ISO, or between 4pm-7pm otherwise, and fully charges from 2am to 5am every day. Benchmark 2 is a deterministic scheduling optimization that does not consider ancillary service markets

$$
\begin{aligned}
&\min_{P_t^{\mathrm{C}}, P_t^{\mathrm{D}}, P_t^{\mathrm{N}}, \mu_t, E_t^{\mathrm{B}}} J^E + J^{\mathrm{DC}} + J^{\mathrm{BD}} \\
&\qquad \text{s.t. } (1) - (15)
\end{aligned}
\tag{47}
$$

Since the BESS does not provide any ancillary services, there is no uncertainty within the BESS's SoC and the objective function is deterministic.

Fig. 1 illustrates the BESS's SoC E_t^{B} and net power $P_{t,d}^{\mathrm{N}}$ under RLABS on the 4th day, when the BESS's full capacity

[1] $\overline{P}^{\mathrm{C}} = \overline{P}^{\mathrm{D}} = 0.15$ MW, $\underline{E}^{\mathrm{B}} = 0.05$ MWh, $\overline{E}^{\mathrm{B}} = 0.45$ MWh, $\eta_c = \eta_d = 0.95$, $\pi^{\mathrm{E}} = 61.82$ \$/MWh, $\pi^{\mathrm{DC}} = 300$ \$/MW, $\pi^{\mathrm{BD}} = 12.5$ \$/MW, $\underline{s} = -0.82$, $\overline{s} = 0.7$, $\tilde{s} = 0$, $\underline{r} = 0$, $\overline{r} = 0.5$, $\tilde{r} = 0.001$.

TABLE I: Monthly Cost from Each Algorithm

	Benchmark 1	Benchmark 2	RLABS
Total cost	\$18,710	\$18,420	\$17,960
Sum of J^{E}	\$15,660	\$15,660	\$15,650
Demand charge	\$2,982	\$2,700	\$2,890
Sum of J^{AC}	-	-	\$620
Sum of J^{BD}	\$71.94	\$61.88	\$48.04

is called upon (at 4pm-5pm), and the 7th day when it is not. The hours when the net power consumption $P_{t,d}^{\mathrm{N}}$ fluctuates are when the BESS is providing frequency regulation. The proposed robust approach did not offer to the frequency regulation market before 4pm on the 4th day to prepare to be fully charged at 4pm. However, it made an offer to the frequency regulation market every hour on the 7th day to maximize the revenue. We also verified that the bounds on the BESS's SoC E_t (5) under our proposed algorithm hold for all the time steps, which shows its robustness.

Table I demonstrates the sum of the cost components J^{E}, J^{AC}, and J^{BD} during a month under each algorithm and the actual monthly demand charge that is the maximum imported power P_t^{G} multiplied by the unit price $3,785$ \$/MW. Overall, the total monthly cost of RLABS is much lower than the benchmarks. The monthly demand charge is higher under RLABS than Benchmark 2 due to the net power fluctuation when providing frequency regulation service. However, the revenues from the ancillary service markets J^{AC} exceeds the excessive amount of the demand charge. Also, the BESS's SoC does not cycle a lot under RLABS and hence the battery degradation cost was the lowest.

V. Conclusion

In this paper, we proposed RLABS that makes offers to the ancillary service markets when the BESS has already been committed to a long-term capacity market. The proposed algorithm makes a valid offer to the frequency regulation market and synchronized reserve markets and is robust against the uncertainties within the frequency regulation and utilization rate. Numerical experiments show the robustness of RLABS as well as its superior performance compared to the two benchmarks.

In our future research, we aim to enhance the conservatism of RLABS by leveraging a more advanced real-time BESS control algorithm or incorporating hour-ahead planning.

References

[1] B. Xu, Y. Wang, Y. Dvorkin, R. Fernández-Blanco, C. A. Silva-Monroy, J.-P. Watson, and D. S. Kirschen, "Scalable planning for energy storage in energy and reserve markets," *IEEE Trans. Power System*, vol. 32, no. 6, pp. 4515–4527, 2017.

[2] K. Garifi, K. Baker, B. Touri, and D. Christensen, "Stochastic model predictive control for demand response in a home energy management system," in *2018 IEEE PESGM*, 2018, pp. 1–5.

[3] G. He, Q. Chen, C. Kang, Q. Xia, and K. Poolla, "Cooperation of wind power and battery storage to provide frequency regulation in power markets," *IEEE Trans. Power Systems*, vol. 32, no. 5, pp. 3559–3568, 2016.

[4] A. A. Thatte, L. Xie, D. E. Viassolo, and S. Singh, "Risk measure based robust bidding strategy for arbitrage using a wind farm and energy storage," *IEEE Trans. Smart Grid*, vol. 4, no. 4, pp. 2191–2199, 2013.

[5] S. Hanif, M. J. E. Alam, K. Roshan, B. A. Bhatti, and J. C. Bedoya, "Multi-service battery energy storage system optimization and control," *Applied Energy*, vol. 311, p. 118614, 2022.

[6] Y. Ji, Q. Xu, J. Zhao, Y. Yang, and L. Sun, "Day-ahead and intra-day optimization for energy and reserve scheduling under wind uncertainty and generation outages," *Electric Power Systems Research*, vol. 195, p. 107133, 2021.

[7] Y. Shi, B. Xu, D. Wang, and B. Zhang, "Using battery storage for peak shaving and frequency regulation: Joint optimization for superlinear gains," *IEEE Trans. Power Systems*, vol. 33, no. 3, pp. 2882–2894, 2017.

[8] H. Zhang, Z. Hu, E. Munsing, S. J. Moura, and Y. Song, "Data-driven chance-constrained regulation capacity offering for distributed energy resources," *IEEE Trans. Smart Grid*, vol. 10, no. 3, pp. 2713–2725, 2018.

[9] A. Ben-Tal and A. Nemirovski, "Robust convex optimization," *Mathematics of operations research*, vol. 23, no. 4, pp. 769–805, 1998.

[10] N. Nazir and M. Almassalkhi, "Guaranteeing a physically realizable battery dispatch without charge-discharge complementarity constraints," *IEEE Trans. Smart Grid*, vol. 14, no. 3, pp. 2473–2476, 2023.

[11] O. Mangasarian, "Absolute value programming," *Computational optimization and applications*, vol. 36, pp. 43–53, 2007.

[12] PJM, "RTO regulation signal data for 2020.xls," https://www.pjm.com/markets-and-operations/ancillary-services.aspx, accessed: 2023-06-28.

[13] L. Wald, M. Albuisson, C. Best, C. Delamare, D. Dumortier, E. Gaboardi, *et al.*, "Soda: a project for the integration and exploitation of networked solar radiation databases." in *Environmental Communication in the Information Society*. International Society for Environmental Protection, Vienna, Austria, 2002, pp. 713–720.

[14] PJM, "Data miner," https://dataminer2.pjm.com/list, accessed: 2023-06-20.

Appendix

A. Lagrange dual functions

The Lagrange dual functions $g_t^{\mathrm{l}}(\boldsymbol{\lambda}_t^{\mathrm{l}})$ of $\min_{\boldsymbol{w}\in\mathcal{W}} E_t^{\mathrm{l}}$ can be derived as follows

$$\begin{aligned}
g_t^{\mathrm{l}}\left(\boldsymbol{\lambda}_t^{\mathrm{l}}\right) = \inf_{\boldsymbol{w}\in\mathcal{W}}\ & E_t^{\text{init}} + \sum_{k=i(t)}^{t-1} \eta_c \left(P_k^{\mathrm{B}} - s_k P_k^{\mathrm{FR}} - r_k P_k^{\mathrm{SR}}\right) \\
& - \sum_{k=i(t)}^{t-1} \left(\frac{1}{\eta_d} - \eta_c\right) P_k^{\mathrm{U}} + \sum_{k=1}^{t-1} \Bigg(\lambda_{t,k}^{\mathrm{l},1}\left(-s_k + \underline{s}\right) + \lambda_{t,k}^{\mathrm{l},2}\left(s_k - \overline{s}\right) \\
& + \lambda_{t,k}^{\mathrm{l},3}\left(-\sum_{l=1}^{k} s_l + \underline{\Gamma}_k^{\mathrm{s}}\right) + \lambda_{t,k}^{\mathrm{l},4}\left(\sum_{l=1}^{k} s_l - \overline{\Gamma}_k^{\mathrm{s}}\right) \\
& + \lambda_{t,k}^{\mathrm{l},5}\left(-r_k + \underline{r}\right) + \lambda_{t,k}^{\mathrm{l},6}\left(r_k - \overline{r}\right) \\
& + \lambda_{t,k}^{\mathrm{l},7}\left(-\sum_{l=1}^{k} r_l + \underline{\Gamma}_k^{\mathrm{r}}\right) + \lambda_{t,k}^{\mathrm{l},8}\left(\sum_{l=1}^{k} r_l - \overline{\Gamma}_k^{\mathrm{r}}\right) \Bigg)
\end{aligned} \tag{48}$$

where $\lambda_{t,k}^{\mathrm{l},j}$ are the Lagrange multipliers composing $\boldsymbol{\lambda}_t^{\mathrm{l}}$, and E_t^{init} and $i(t)$ are defined as follows.

$$E_t^{\text{init}} = \begin{cases} E_1^{\mathrm{B}} & \text{if } t < t_{\mathrm{F}} \\ \overline{E}^{\mathrm{B}} & \text{if } t \geq t_{\mathrm{F}} \end{cases},\quad i(t) = \begin{cases} 1 & \text{if } t < t_{\mathrm{F}} \\ t_{\mathrm{F}} & \text{if } t \geq t_{\mathrm{F}}. \end{cases} \tag{49}$$

Considering that $g_t^{\mathrm{l}}(\boldsymbol{\lambda}_t^{\mathrm{l}})$ is equal to $-\infty$ if one of the coefficients of s_k and r_k is non-zero, we get the following

$$g_t^{\mathrm{l}}\left(\boldsymbol{\lambda}_t^{\mathrm{l}}\right) = \begin{cases} E_t^{\text{init}} + \sum_{k=i(t)}^{t-1} \eta_c P_k^{\mathrm{B}} & \\ \quad - \left(\frac{1}{\eta_d} - \eta_c\right) P_k^{\mathrm{U}} + \Omega_t^{\mathrm{l}} & \text{if } \boldsymbol{\lambda}_t^{\mathrm{l}} \in \Lambda_t^{\mathrm{l}} \\ -\infty & \text{otherwise} \end{cases} \tag{50}$$

where Ω^{l}_t and Λ^{l}_t are defined as follows

$$\Omega^{\mathrm{l}}_t = \sum_{k=i(t)}^{t-1} \lambda^{\mathrm{l},1}_{t,k}\underline{s} - \lambda^{\mathrm{l},2}_{t,k}\overline{s} + \lambda^{\mathrm{l},3}_{t,k}\underline{\Gamma}^{\mathrm{s}}_k - \lambda^{\mathrm{l},4}_{t,k}\overline{\Gamma}^{\mathrm{s}}_k + \lambda^{\mathrm{l},5}_{t,k}\underline{r} - \lambda^{\mathrm{l},6}_{t,k}\overline{r} + \lambda^{\mathrm{l},7}_{t,k}\underline{\Gamma}^{\mathrm{r}}_k - \lambda^{\mathrm{l},8}_{t,k}\overline{\Gamma}^{\mathrm{r}}_k \tag{51}$$

$$\begin{aligned}\Lambda^{\mathrm{l}}_t := \Bigg\{ \boldsymbol{\lambda}^{\mathrm{l}}_t \Bigg| & -\eta P^{\mathrm{FR}}_k - \lambda^{\mathrm{l},1}_{t,k} + \lambda^{\mathrm{l},2}_{t,k} - \sum_{l=k}^{t-1} \lambda^{\mathrm{l},3}_{t,l} - \lambda^{\mathrm{l},4}_{t,l} = 0 \\ & -\eta P^{\mathrm{SR}}_k - \lambda^{\mathrm{l},5}_{t,k} + \lambda^{\mathrm{l},6}_{t,k} - \sum_{l=k}^{t-1} \lambda^{\mathrm{l},7}_{t,l} - \lambda^{\mathrm{l},8}_{t,l} = 0 \\ & \qquad \forall k \in \{i(t), \ldots, t-1\} \\ & -\lambda^{\mathrm{l},1}_{t,k} + \lambda^{\mathrm{l},2}_{t,k} - \sum_{l=1}^{k} \lambda^{\mathrm{l},3}_{t,l} - \lambda^{\mathrm{l},4}_{t,l} = 0 \\ & -\lambda^{\mathrm{l},5}_{t,k} + \lambda^{\mathrm{l},6}_{t,k} - \sum_{l=1}^{k} \lambda^{\mathrm{l},7}_{t,l} - \lambda^{\mathrm{l},8}_{t,l} = 0 \forall k \in \{1, \ldots, i(t)-1\} \Bigg\}\end{aligned}$$

Likewise, the function $g^{\mathrm{u}}_t(\lambda^{\mathrm{u}}_t)$ is given as follows

$$g^{\mathrm{u}}_t\left(\boldsymbol{\lambda}^{\mathrm{u}}_t\right) = \begin{cases} E^{\mathrm{init}}_t + \sum_{k=i(t)}^{t-1} \eta P^{\mathrm{B}}_k + \Omega^{\mathrm{u}}_t & \text{if } \boldsymbol{\lambda}^{\mathrm{u}}_t \in \Lambda^{\mathrm{u}}_t \\ -\infty & \text{otherwise} \end{cases} \tag{52}$$

where Ω^{u}_t and Λ^{u}_t are defined as (51) and (52) with $\lambda^{\mathrm{l},j}_{t,k}$ alternated to $-\lambda^{\mathrm{u},j}_{t,k}$ and η_c alternated to η.